# Stabilization of Almost Periodic Piecewise Linear Systems with Norm-Bounded Uncertainty for Roll-to-Roll Dry Transfer Manufacturing Processes

C. Martin, W. Li, and D. Chen, Member, IEEE

Abstract—This paper presents the first stabilization result for almost periodic piecewise linear systems (APPLSs) with both norm-bounded additive modeling uncertainty and dwell-time uncertainty. The technique employs a mixed-mode time-varying Lyapunov function to generate a sequence of controller gains that stabilize the uncertain APPLS. This modelling structure aligns with the R2R dry transfer of patterned two-dimensional (2D) materials, an emerging technology for continuous, chemical-free flexible material and device transfer. Thus, the proposed controller synthesis method provides stabilization guarantees for a novel modeling framework with applications in the expanding realm of advanced 2D device manufacturing.

# Index Terms – Periodic systems, dwell-time uncertainty, modeling uncertainty, exponential stability

#### I. INTRODUCTION

Roll-to-roll (R2R) manufacturing involves processing thin films using a series of rollers [1]. Over the past two decades, it has been extensively used to fabricate flexible electronic components and advanced two-dimensional (2D) materials [2]. A critical procedure in R2R manufacturing is transferring the product from the substrate that it is grown on to a target one for its end-use application. This transfer process is often batch-style and discrete, which can hinder throughput relative to fully continuous processes [3]. To address this issue, continuous R2R-compatible transfer processes for 2D materials, especially graphene, have been developed. However, they suffer from drawbacks such as the use of toxic chemical etchants and slow delamination speeds [4].

The R2R dry transfer process offers a promising solution to the transfer issue, enabling high-quality 2D material transfer at a high throughput without using chemical etchants [5]–[7]. This method involves sandwiching the 2D material between the donor (typically the growth) substrate and the target substrate. The stack passes through nipping rollers and is peeled apart in such a way that the 2D material adheres to the target and delaminates from the donor substrate. Successful transfer relies on maintaining optimal peeling conditions, including desired web tension and web speed values [6], [7].

2D materials often exhibit patterns, as exemplified in [6] and [7], where  $10 \text{ cm} \times 10 \text{ cm}$  CVD graphene samples grown on copper foil are spaced regularly on a carrier web and then transferred to a polymer substrate, creating a peeling pattern. In addition to graphene transfer, the 2D material itself may have patterns, as in [8], where patterned MoS<sub>2</sub> strips are peeled from their silicon substrate. When a peeling process has

sections with different material properties, these abrupt changes between modes naturally create a piecewise modeling structure. If these sections follow a predictable pattern with an error margin, the dry transfer process can be formulated as a periodic piecewise system with bounded dwell-time uncertainty, where dwell-time is the amount of time between mode switches.

In addition, each mode in the R2R dry transfer of patterned 2D materials can be represented as a linear system with additive, unstructured uncertainty. This modeling approach involves using the web tensions and velocities near a desired trajectory to build linear differential inclusion (LDI) system representations for each mode [9]-[11]. Then, bounding ellipse techniques can be used to represent each mode as a linear system with additive, unstructured, norm-bounded uncertainty [12]-[15]. This method elegantly integrates bounds on modeling errors and nonlinearities into a convex uncertainty structure that can be used to achieve the desired control performance with reduced computational cost. A similar method was used to bound the dynamics of R2R dry transfer systems without patterning within a polytopic uncertainty set [16]. Thus, to regulate the R2R dry transfer process, control tools for periodic piecewise linear systems (PPLSs) with dwell-time uncertainty and norm-bounded modeling uncertainty need to be developed.

Deterministic PPLSs, defined as systems with a set of modes with linear dynamics and a predetermined, periodic switching signal between them, have been intensively investigated [17]-[19]. Maintaining switching stability is the essential first step to controlling PPLSs. Stabilizing controllers have been developed for deterministic PPLSs using mode dependent Lyapunov functions [18], [19]. These PPLS stabilization techniques have been generalized to PPLSs with mode-dependent additive norm-bounded uncertainty [20]. In addition, the PPLS modeling structure has been extended to almost periodic piecewise linear systems (APPLSs) that consider bounded dwell-time uncertainty [21]. This extension applies to systems where the switching sequence is known and periodic, but each switching time is only guaranteed to occur within a pre-defined time interval. While stabilization results have been developed for APPLSs with deterministic dynamics, the challenge of guaranteeing the stability of APPLSs with modeling uncertainty has not been treated [21].

To address this challenge, this study uses a mixed-mode time-varying Lyapunov function technique to prove that a precalculated set of switched state feedback controllers stabilize

This work is based upon work supported primarily by the National Science Foundation under Cooperative Agreement No. EEC-1160494 and CMMI-2041470.

The authors are with the Walker Department of Mechanical Engineering, the University of Texas at Austin, TX 78712, USA. Corresponding author's email: cbmartin129@utexas.edu (C. Martin)

APPLSs with norm-bounded modeling and dwell time uncertainties. A practical controller synthesis algorithm is presented along with the theoretical result. This method is innovative in that, to the best of our knowledge, this is the first published stabilization result for APPLSs with both normbounded modeling and dwell time uncertainty. Additionally, the sequence of stabilizing controller gains is formulated with the knowledge that the exact switching times, within given bounds, are unknown a-priori but can be measured in real time. Utilizing this online measurement information enables more precise stabilization of the switched system than existing research on APPLSs [21]. This information structure aligns with the R2R dry transfer system, where the switching times are only known beforehand to exist within bounded intervals, yet the switching events can be measured in real-time.

The paper is organized as follows. Section IIA presents the APPLS with norm-bounded modeling uncertainty and dwell-time uncertainty, while IIB presents the stabilizing controller synthesis result. Section IIIA summarizes the R2R dry transfer system dynamics, IIIB formulates the system as an APPLS with bounded modeling and dwell-time uncertainty, and IIIC presents simulation results using the proposed controller to stabilize the R2R dry transfer of CVD-grown graphene. Concluding thoughts are provided in Section IV.

# II. STABILIZATION OF APPLSS WITH BOUNDED MODELING AND DWELL-TIME UNCERTAINTY

## A. APPLS Problem Formulation

Let there be an APPLS with norm-bounded modeling uncertainty, bounded dwell-time uncertainty, S modes with a known switching sequence, and a set of state feedback gains defined as follows. For  $t \in [lT_P^* + t_{l,i-1}, lT_P^* + t_{l,i})$ ,

$$\dot{x}(t) = A_i x(t) + B_i u(t) + F_i \pi(t), \tag{1}$$

$$\pi(t)^T \pi(t) \le \left( G_i x(t) \right)^T \left( G_i x(t) \right). \tag{2}$$

Additionally.

$$u(t) = \begin{cases} K_{l}x(t), t \in \left[lT_{P}^{*} + \overline{t_{l-1}}, lT_{P}^{*} + \underline{t_{i}}\right) \\ K_{l,i+1}x(t), t \in \left[lT_{P}^{*} + \underline{t_{i}}, lT_{P}^{*} + t_{l,i}\right) \\ K_{l+1,i+1}x(t), t \in \left[lT_{P}^{*} + t_{l,i}, lT_{P}^{*} + \overline{t_{i}}\right) \end{cases}$$
(3)

In (1)-(3),  $x(t) \in \mathbb{R}^n$  is the state variable and  $\pi(t) \in \mathbb{R}^{n_p}$ contains the unstructured uncertainty in (2).  $A_i \in \mathbb{R}^{n \times n}$  and  $B_i \in \mathbb{R}^{n \times n_u}$  are the nominal linear dynamics of the  $i^{th}$  mode, and  $K_i$ ,  $K_{i,i+1}$ , and  $K_{i+1,i+1}$  are the state feedback gains associated with the three mode-dependent time segments in (3). Define  $A_{cl_{i,i}} = A_i + B_i K_i$ ,  $A_{cl_{i,i+1}} = A_i + B_i K_{i,i+1}$ , and  $A_{cl_{i+1,i+1}} = A_{i+1} + B_{i+1}K_{i+1,i+1}$  as the switched closed-loop nominal linear dynamics.  $F_i$  and  $G_i$  are the weights of the additive norm-bounded uncertainty of the  $i^{th}$  mode.  $T_P^*$  is the fundamental period of the system, and  $lT_P^* + t_{l,i}$  is the actual switching instant from the  $i^{th}$  to the  $(i+1)^{th}$  mode in the  $l^{th}$ period.  $lT_P^* + t_i$  is the lower bound on that switching instant and  $lT_P^* + \overline{t_i}$  is the upper bound. Since the system is periodic,  $lT_P^* + t_{l,S}$  represents the switching instant from the  $S^{th}$  mode to the 1<sup>st</sup> mode. Let  $T_i = \underline{t_i} - \overline{t_{i-1}}$  and  $T_{i,i+1} = \overline{t_i} - \underline{t_i}$ . The switching rule defined for the APPLS in (1)-(3) is illustrated

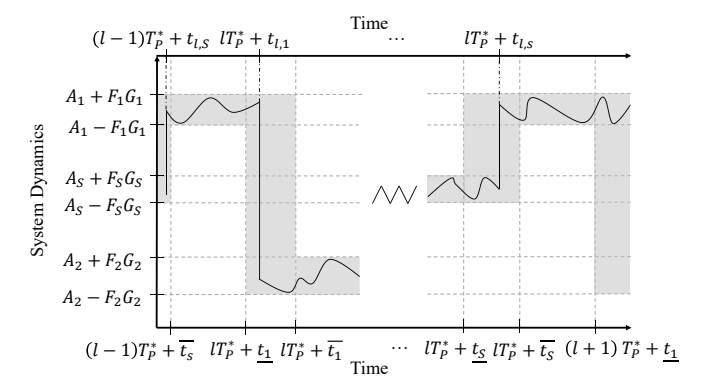


Figure 1. A 1D APPLS with bounded dwell-time and modeling uncertainty for a 1-dimensional system in Figure 1. In the figure, the grey shaded regions represent admissible system dynamics at a given time, while the solid black line is an example trajectory.

Remark 1: The presented almost periodic switching structure combines time segments with known active subsystems and transitional segments where switching between subsystems occurs [21]. This study considers the effect of adding modeling uncertainty with the structure represented in (2) to that formulation.

#### B. Stabilization

The main objective of this study, a set of stabilizing controller gains for APPLSs with norm-bounded modeling and dwell-time uncertainty, is developed in Theorem 1.

**Theorem 1:** Consider the following mixed-mode time-varying Lyapunov function for system (1)-(3),

$$V(t) = x(t)^T P(t)x(t), \tag{4}$$

$$P(t) = \begin{cases} P_i & t \in [lT_P^* + \overline{t_{i-1}}, lT_P^* + \underline{t_i}) \\ P_{i,i+1} & t \in [lT_P^* + \underline{t_i}, lT_P^* + \overline{t_i}). \end{cases}$$
 (5)

Additionally, define the following matrix function:

$$\mathbf{M}(\Omega, \Psi, \Upsilon, \Xi, \rho, \omega) = \begin{bmatrix} \mathbf{sym}(\Omega) + \omega \Psi \Psi^T + \rho \Upsilon & \Xi^T \\ \Xi & -\omega \mathbf{I} \end{bmatrix}$$
(6)

where  $sym(\Omega)$  denotes  $\Omega + \Omega^T$ . Let there be  $\alpha_i \ge 0$ ,  $\beta_i \ge 0$ ,  $\gamma_i \ge 0$ ,  $Q_i > 0$ ,  $Q_{i,i+1} > 0$ ,  $Y_i$ ,  $Y_{i,i+1}$ ,  $Y_{i+1,i+1}$  and given constants  $\lambda_i$ ,  $\lambda_{i,i+1}$ ,  $\mu_i$ , and  $\mu_{i,i+1}$  such that,

$$\mathbf{M}(A_i Q_i + B_i Y_i, F_i, Q_i, G_i Q_i, \lambda_i, \alpha_i) < 0 \tag{7}$$

$$M(A_i Q_{i,i+1} + B_i Y_{i,i+1}, F_i, Q_{i,i+1}, G_i Q_{i,i+1}, \lambda_{i,i+1}, \beta_i) < 0 \quad (8)$$

 $M(A_{i+1}Q_{i,i+1} +$ 

$$B_{i+1}Y_{i+1,i+1}, F_{i+1}, Q_{i,i+1}, G_{i+1}Q_{i,i+1}, \lambda_{i,i+1}, \gamma_i) < 0$$
(9)

$$Q_{S,S+1} \le \mu_1 Q_1 \tag{10}$$

$$Q_{i-1,i} \le \mu_i Q_i \tag{11}$$

$$Q_i \le \mu_{i,i+1} Q_{i,i+1} \tag{12}$$

$$\sum_{i=1}^{S} \lambda_i T_i + \lambda_{i,i+1} T_{i,i+1} - \ln \mu_i - \ln \mu_{i,i+1} \ge 2\lambda^* T_P^*. \tag{13}$$

Then, system (1)-(3) is  $\lambda^*$ -exponentially stable with  $K_i = Y_i Q_i^{-1}$ ,  $K_{i,i+1} = Y_{i,i+1} Q_{i,i+1}^{-1}$ , and  $K_{i+1,i+1} = Y_{i+1,i+1} Q_{i,i+1}^{-1}$ .

**Proof.** Equations (7)-(9) imply the following,

$$\mathbf{M}\left(P_{i}A_{cl_{i,i}}, G_{i}^{T}, P_{i}, F_{i}^{T}P_{i}, \lambda_{i}, a_{i}\right) < 0 \tag{14}$$

$$M(P_{i,i+1}A_{cl_{i,i+1}}, G_i^T, P_{i,i+1}, F_i^T P_{i,i+1}, \lambda_{i,i+1}, b_i) < 0$$
 (15)

$$M(P_{i,i+1}A_{cl_{i+1,i+1}}, G_{i+1}^{T}, P_{i,i+1}, F_{i+1}^{T}P_{i,i+1}, \lambda_{i,i+1}, c_{i}) < 0$$

where  $P_i = Q_i^{-1}$ ,  $P_{i,i+1} = Q_{i,i+1}^{-1}$ ,  $a_i = 1/\alpha_i$ ,  $b_i = 1/\beta_i$ ,  $c_i = 1/\gamma_i$ . In addition, (10)-(12) imply the following,

$$P_1 \le \mu_1 P_{S,S+1} \tag{17}$$

$$P_i \le \mu_i P_{i-1,i} \tag{18}$$

$$P_{i,i+1} \le \mu_{i,i+1} P_i. \tag{19}$$

Equation (15), in turn, implies the following. For  $t \in [lT_P^* + t_i, lT_P^* + t_{l,i})$ ,

$$\dot{V} = sym(x(t)^T P_{i,i+1} A_{cl_{i,i+1}} x(t)) + 2x(t)^T P_{i,i+1} F_i \pi(t)$$

$$\leq x(t)^{T} \left( sym \left( P_{i,i+1} A_{cl_{i,i+1}} \right) + b_{i} G_{i}^{T} G_{i} + \lambda_{i,i+1} P_{i,i+1} \right) x(t) + 2x(t)^{T} P_{i,i+1} F_{i} \pi(t) - b_{i} \pi(t)^{T} \pi(t) - \lambda_{i,i+1} V(t) \leq -\lambda_{i,i+1} V(t).$$
 (20)

Analogously, (16) implies, for  $t \in [lT_P^* + t_{l,i}, lT_P^* + \overline{t_i})$ ,

$$\dot{V} \le -\lambda_{i,i+1} V(t). \tag{21}$$

Thus, for  $t \in [lT_P^* + t_i, lT_P^* + \overline{t_i})$ ,

$$\dot{V} \le -\lambda_{i,i+1} V(t). \tag{22}$$

By similar logic, (14) implies, for  $t \in [lT_P^* + \overline{t_{i-1}}, lT_P^* + t_i)$ ,

$$\dot{V} \le -\lambda_i V(t). \tag{23}$$

Additionally, (17)-(19) imply the following inequalities,

$$V\left(lT_{P}^{*} + \overline{t_{S}}\right) \le \mu_{1}e^{-\lambda_{S,S+1}T_{S,S+1}}V\left(lT_{P}^{*} + t_{S}\right) \tag{24}$$

$$V\left(lT_{P}^{*} + \overline{t_{i}}\right) \le \mu_{i+1}e^{-\lambda_{i,i+1}T_{i,i+1}}V\left(lT_{P}^{*} + \underline{t_{i}}\right) \tag{25}$$

$$V\left(lT_{P}^{*}+t_{i}\right)\leq\mu_{i,i+1}e^{-\lambda_{i}T_{i}}V\left(lT_{P}^{*}+\overline{t_{i-1}}\right)\tag{26}$$

Equations (22)-(26) then imply,

$$V(lT_{P}^{*} + \overline{t_{S}}) \leq \mu_{1}e^{-\lambda_{S,S+1}T_{S,S+1}}\mu_{S,S+1}e^{-\lambda_{S}T_{S}}V(lT_{P}^{*} + \overline{t_{S-1}})$$

$$\leq (\prod_{i=1}^{S} \mu_{i}\mu_{i+1})e^{-\sum_{i=1}^{S} \lambda_{i}T_{i} + \lambda_{i,i+1}T_{i,i+1}}V((l-1)T_{P}^{*} + \overline{t_{S}})$$

$$< e^{-l\sum_{i=1}^{S} \lambda_{i}T_{i} + \lambda_{i,i+1}T_{i,i+1} - \ln \mu_{i} - \ln \mu_{i,i+1}V(\overline{t_{S}})}$$
(27)

Thus, by (13),

$$V(lT_P^* + \overline{t_S}) \le e^{-l2\lambda^* T_P^*} V(\overline{t_S}). \tag{28}$$

In addition, since  $V(\overline{t_S}) = x(\overline{t_S})^T P(\overline{t_S}) x(\overline{t_S})$  and  $V(lT_P^* + \overline{t_S}) = x(lT_P^* + \overline{t_S})^T P(\overline{t_S}) x(lT_P^* + \overline{t_S})$ ,

$$\|x(lT_P^* + \overline{t_S})\| \le \sqrt{\frac{\overline{\lambda}(P(\overline{t_S}))}{\underline{\lambda}(P(\overline{t_S}))}} e^{-\lambda^* lT_P^*} \|x(\overline{t_S})\|.$$
 (29)

Thus, the state norm at the end of each period decreases exponentially. Next, we show that the state norm within each

period is exponentially bounded. By Coppel's inequality [22], [23], the following relationships can be guaranteed,

$$||x(t)|| \le ||x(lT_P^* + \overline{t_{i-1}})|| \exp\left(\int_{lT_P^* + \overline{t_{i-1}}}^t \mu\left(A_{cl_{i,i}} + F_i\Delta(\tau)G_i\right)d\tau\right), t \in [lT_P^* + \overline{t_{i-1}}, lT_P^* + \underline{t_i})$$

$$(30)$$

$$||x(t)|| \le ||x(lT_P^* + \underline{t_i})|| \exp\left(\int_{lT_P^* + \underline{t_i}}^t \mu(A_{cl_{i,i+1}} + F_i\Delta(\tau)G_i)d\tau\right), t \in [lT_P^* + t_i, lT_P^* + t_{l,i})$$
(31)

$$||x(t)|| \le ||x(lT_P^* + t_{l,i})|| \exp\left(\int_{lT_P^* + t_{l,i}}^t \mu(A_{cl_{i+1,i+1}} + F_{i+1}\Delta(\tau)G_{i+1})d\tau\right), t \in [lT_P^* + t_{l,i}, lT_P^* + \overline{t_i}),$$
(32)

where  $\|\Delta(t)\| \le 1$  is a compact way to represent the additive, unstructured, norm-bounded uncertainty in (1) and (2). Additionally, according to matrix measure results [22], and noting that  $\mu$  is an operator defined as  $\mu(\Omega) = \frac{1}{2}\bar{\lambda}(\Omega^T + \Omega)$ ,

$$\mu\left(A_{cl_{m,n}}+F_{m}\Delta(t)G_{m}\right)\leq\mu\left(A_{cl_{m,n}}\right)+\|F_{m}\|\|G_{m}\|, \tag{33}$$

where (m,n) = (i, i), (i,i+1), (i+1,i+1). Thus, for  $t \in [lT_P^* + \underline{t_i}, lT_P^* + t_{l,i})$ , (31) and (33) imply the following,

$$||x(t)|| \le ||x(lT_P^* + \underline{t_i})|| \max(1, \exp((\mu(A_{cl_{i,i+1}}) + ||F_i|| ||G_i||)T_{i,i+1})).$$

$$(34)$$

Similarly, for  $t \in [lT_P^* + t_{l,i}, lT_P^* + \overline{t_i})$ , (31)-(33) imply,

$$||x(t)|| \le ||x(lT_P^* + \underline{t_i})|| \max(1, \exp((\mu(A_{cl_{i,i+1}}) + ||F_i|| ||G_i||) T_{i,i+1}), \exp((\mu(A_{cl_{i+1,i+1}}) + ||F_{i+1}|| ||G_{i+1}||) T_{i,i+1})) = ||x(lT_P^* + \underline{t_i})|| \phi_{i,i+1}.$$
(35)

Thus.

$$\sup_{t \in [lT_P^* + \underline{t_i}, lT_P^* + \overline{t_i})} \|x(t)\| \le \phi_{i, i+1} \left\| x \left( lT_P^* + \underline{t_i} \right) \right\| \tag{36}$$

Also, by similar logic,

$$\sup_{t \in [lT_{P}^{*} + \overline{t_{i-1}}, lT_{P}^{*} + \underline{t_{i}})} ||x(t)|| \le \phi_{i} ||x(lT_{P}^{*} + \overline{t_{i-1}})||,$$
 (37)

where  $\phi_i = \max \left(1, \exp\left(\left(\mu\left(A_{cl_{i,i}}\right) + \|F_i\| \|G_i\|\right)T_{i,}\right)\right)$ . Thus,

$$\sup_{t \in [(l-1)T_{P}^{*} + \overline{t_{S}}, lT_{P}^{*} + \underline{t_{1}})} \|x(t)\| \leq \phi_{1} \|x((l-1)T_{P}^{*} + \overline{t_{S}})\|$$

$$\sup_{t \in [lT_{P}^{*} + \underline{t_{1}}, lT_{P}^{*} + \overline{t_{1}})} \|x(t)\| \leq \phi_{1,2} \|x(lT_{P}^{*} + \underline{t_{1}})\| \leq$$

$$\lim_{t \in [lT_{P}^{*} + \underline{t_{1}}, lT_{P}^{*} + \overline{t_{1}})} \|x((l-1)T_{P}^{*} + \overline{t_{S}})\| \dots$$

$$\sup_{t \in [lT_{P}^{*} + \underline{t_{S}}, lT_{P}^{*} + \overline{t_{S}})} \|x(t)\| \leq \prod_{1}^{S} \phi_{i} \phi_{i,i+1} \|x((l-1)T_{P}^{*} + \overline{t_{S}})\|,$$

$$\lim_{t \in [lT_{P}^{*} + \underline{t_{S}}, lT_{P}^{*} + \overline{t_{S}})} \|x(t)\| \leq \lim_{1}^{S} \phi_{i} \phi_{i,i+1} \|x((l-1)T_{P}^{*} + \overline{t_{S}})\|,$$

where, by definition,  $\phi_i$ ,  $\phi_{i,i+1} \ge 1$ . Thus,

$$\begin{split} \sup_{t \in [(l-1)T_{p}^{*} + \overline{t_{S}}, lT_{p}^{*} + \overline{t_{S}})} & \|x(t)\| \leq \max_{i} \sup_{t \in [lT_{p}^{*} + \overline{t_{i-1}}, lT_{p}^{*} + \overline{t_{i}})} \|x(t)\| \\ & \leq \prod_{i=1}^{S} \phi_{i} \phi_{i, i+1} \|x((l-1)T_{p}^{*} + \overline{t_{S}})\|. \end{split} \tag{39}$$

Therefore, for  $t \in [(l-1)T_P^* + \overline{t_S}, lT_P^* + \overline{t_S})$ , we get,

$$\|x(t)\| \leq \prod_{i=1}^{S} \phi_{i} \phi_{i,i+1} \|x((l-1)T_{P}^{*} + \overline{t_{S}})\|$$

$$\leq \prod_{i=1}^{S} \phi_{i} \phi_{i,i+1} \sqrt{\frac{\overline{\lambda}(P(\overline{t_{S}}))}{\underline{\lambda}(P(\overline{t_{S}}))}} e^{-\lambda^{*}(l-1)T_{P}^{*}} \|x(\overline{t_{S}})\|$$

$$\leq \kappa e^{-\lambda^{*}lT_{P}^{*}} \|x(\overline{t_{S}})\|,$$

$$(40)$$

where 
$$\kappa = \prod_{i=1}^{S} \phi_i \phi_{i,i+1} \sqrt{\frac{\overline{\lambda}(P(\overline{t_S}))}{\underline{\lambda}(P(\overline{t_S}))}} e^{\lambda^* T_P^*}$$
. Since  $t - \overline{t_S} \leq lT_P^*$ ,

$$||x(t)|| \le \kappa e^{-\lambda^* l\left(t - \overline{t_S}\right)} ||x\left(\overline{t_S}\right)||,\tag{41}$$

where  $\kappa \geq 1$ ,  $\lambda^* \geq 0$ . Thus, the system is  $\lambda^*$ -exponentially stable.  $\Box$ 

Remark 2: Unlike in previous works, where the switching times are known a-priori [18]–[20] or unmeasurable within the transition regions [21], this study assumes that the switching times are measurable, but unknown a-priori within the transition regions. This information structure enables a tighter exponential convergence bound than is achievable with unmeasurable switching times, and it allows the results to apply to a broader class of applications than when the switching times are exactly pre-determined.

Theorem 1 shows how to guarantee stability for the APPLS defined in (1)-(3) for a given  $\lambda_i$ ,  $\lambda_{i,i+1}$ ,  $\mu_i$ , and  $\mu_{i,i+1}$ . However, determining these constants is non-trivial. In addition, it is desirable for the rate of convergence,  $\lambda^*$ , to be high. The following stabilizing controller design (SCD) algorithm gives a systematic method to design a stabilizing controller with a high  $\lambda^*$  for the APPLS (1)-(3).

**Remark 3:** The weighting factor  $w_{\mu}$  accounts for the  $\ln \mu_i$  terms in (13) using a linear approximation, as minimizing  $\ln \mu_i$  is non-convex.

Algorithm 1, utilizing the stability certification developed in Theorem 1, is the first method that can generate a set of stabilizing state feedback gains for the robust APPLS (1)-(3).

# Algorithm 1: Stabilizing Controller Design (SCD)

Step 1: Given  $\epsilon > 0$ ,  $M_{\lambda} > 0$ ,  $M_{\mu} > 0$ , and  $w_{\mu} > 0$ ;  $\lambda_{i,i+1}^{(0)} = -M_{\lambda}$ ,  $\mu_i^{(0)} = M_{\mu}$ ,  $\mu_{i,i+1}^{(0)} = M_{\mu}$ ,  $\chi^{(0)} = +\infty$ , and k = 1. If (42),  $\lambda_i^{(0)} = 0$ ; Else,  $\lambda_i^{(0)} = -M_{\lambda}$ ; where (42) is,

 $M(A_iQ_i + B_iY_i, F_i, Q_i, G_iQ_i, 0, \alpha_i) < 0.(42)$ 

Step 2: With  $\lambda_i^{(k-1)}$ ,  $\lambda_{i,i+1}^{(k-1)}$ ,  $\mu_i^{(k-1)}$ , and  $\mu_{i,i+1}^{(k-1)}$ ; find  $Q_i^{(k)}$ ,  $Q_{i,i+1}^{(k)}$ ,  $Y_i^{(k)}$ ,  $Y_{i,i+1}^{(k)}$ , and  $Y_{i+1,i+1}^{(k)}$  such that (7)-(12). Step 3: With  $Q_i^{(k)}$ ,  $Q_{i,i+1}^{(k)}$ ,  $Y_i^{(k)}$ ,  $Y_{i,i+1}^{(k)}$ , and  $Y_{i+1,i+1}^{(k)}$ ; find  $\lambda_i^{(k)}$ ,

**Step 3:** With  $Q_i^{(k)}$ ,  $Q_{i,i+1}^{(k)}$ ,  $Y_i^{(k)}$ ,  $Y_{i,i+1}^{(k)}$ , and  $Y_{i+1,i+1}^{(k)}$ ; find  $\lambda_i^{(k)}$ ,  $\lambda_{i,i+1}^{(k)}$ ,  $\mu_i^{(k)}$ , and  $\mu_{i,i+1}^{(k)}$  that minimize  $\chi^{(k)} = -\sum_{i=1}^{S} \left(\lambda_i^{(k)} T_i + \lambda_{i,i+1}^{(k)} T_{i,i+1} - w_\mu \left(\mu_i^{(k)} + \mu_{i,i+1}^{(k)}\right)\right)$  subject to (7)-(12).

Step 4: If  $|\chi^{(k)} - \chi^{(k-1)}| < \epsilon$ : STOP. Else: Set k = k + 1, return to Step 2.

**Step 5:** Using  $\lambda_i^{(k)}$ ,  $\lambda_{i,i+1}^{(k)}$ ,  $\mu_i^{(k)}$ , and  $\mu_{i,i+1}^{(k)}$ ; if  $\lambda^* > 0$  according to (13), then  $Q_i^{(k)}$ ,  $Q_{i,i+1}^{(k)}$ ,  $Y_i^{(k)}$ ,  $Y_{i,i+1}^{(k)}$ , and  $Y_{i+1,i+1}^{(k)}$  can be used to build a set of stabilizing controller gains.

## III. R2R DRY TRANSFER EXAMPLE

The usefulness of Algorithm 1 will be demonstrated by applying it to stabilize web tension and velocity in the R2R dry transfer system for patterned flexible devices and materials.

# A. R2R Dry Transfer Dynamic System Model

First, the dynamics of the R2R dry transfer system, as formulated in [24] and [25], will be presented here in the context of patterned peeling. The system is illustrated in Figure 2, and the key physical parameters are listed in Table I.

The R2R dry transfer process has two sets of dynamics connected through the web tensions: the web transfer dynamics dominated by the rewinding rollers, and the peeling front dynamics dominated by an energy balance. When peeling is occurring, and neglecting higher-order terms, the constraint on the three web tensions due to the energy balance at the peeling front can be summarized as follows [24]:

$$t_2 + t_3 - t_1 = \tau_i, (43)$$

where  $\tau_i$ , a pattern section-dependent parameter, is defined,

$$\tau_i = b\Gamma_i - \frac{1}{2} \left[ E_2 I_{2,i} \left( K_1^2 - K_2^2 \right) + E_3 I_{3,i} \left( K_1^2 - K_3^2 \right) \right]. \tag{44}$$

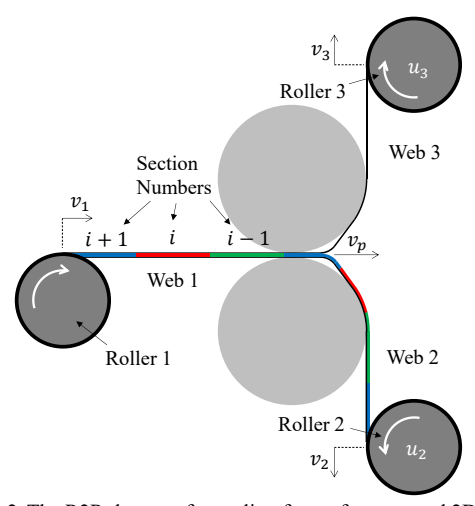


Figure 2. The R2R dry transfer peeling front of a patterned 2D material

TABLE I. KEY R2R DRY TRANSFER PARAMETERS

Symbol	Meaning			
$t_j, j = 1, 2, 3$	Tension in web $j$ (N)			
$v_j$ , $j = 1, 2, 3$	Velocity of web $j$ (m/s)			
$l_j, j = 1, 2, 3$	Unstretched length web $j$ (m)			
$\varepsilon_j$ , $j = 1, 2, 3$	Strain in web j (m/m)			
$u_j, j = 2, 3$	Motor torque inputs (N-m)			
$v_p$	Peeling front velocity (m/s)			
$K_j, j = 1, 2, 3$	Bending Curvature of web <i>j</i> (1/m)			
$E_j, j = 1, 2, 3$	Elastic Modulus of web j (N/m²)			
$Ar_j, j = 1, 2, 3$	Cross-sectional Area of web j (m <sup>2</sup> )			
$R_j$ , $j = 1, 2, 3$	Radius of roller j (m)			
$J_j$ , $j = 1, 2, 3$	Moment of inertia roller j (kg-m²)			
$f_j$ , $j = 1, 2, 3$	Friction coefficient of roller <i>j</i> (m/s)			
b	Width of the contact surface (m)			
Pattern Section-Dependent Parameters				
$I_{j,i}, j = 1, 2, 3$	Moment of Inertia of web $j$ section $i$ (m <sup>4</sup> )			
$\Gamma_i$	Adhesion Energy of section i (J/m²)			

In this study,  $\tau_i$  will be treated as a constant parameter. Then, the web dynamics can be defined accordingly:

$$\dot{v}_j(t) = -\frac{R_j^2}{J_j}t_j(t) + \frac{R_j}{J_j}u_j(t) - \frac{f_j}{R_j}v_j(t), j = 2, 3, \tag{45}$$

$$\dot{t}_{j} = \frac{\partial t_{j}}{\partial l_{1}}(t) \cdot \dot{l_{1}} + \frac{\partial t_{j}}{\partial l_{2}}(t) \cdot \dot{l_{2}} + \frac{\partial t_{j}}{\partial l_{3}}(t) \cdot \dot{l_{3}}, \ j = 2, 3, \tag{46}$$

$$\dot{l}_1(t) = \frac{v_1(t) - v_p(t)}{1 + \varepsilon_1(t)}, \, \dot{l}_j(t) = \frac{v_p(t)}{1 + \varepsilon_1(t)} - \frac{v_j(t)}{1 + \varepsilon_j(t)}, \, j = 2, 3$$
 (47)

where  $\varepsilon_j = \frac{t_j}{Ar_j E_j}$ . The partial derivatives  $\frac{\partial t_j}{\partial l_k}$  can be defined numerically [16], [25].

Thus, (43)-(47) define a piecewise nonlinear, state-space model of the R2R dry transfer system for patterned materials. These equations can be written in the following form. When section i is being peeled,

$$\dot{x} = f_i(x, w, u), \ x = [v_2, v_3, t_2, t_3]^T, w = v_p, u = [u_2, u_3]^T, \ y = [v_2, v_3, t_1, t_2, t_3]^T,$$
(48)

where it is assumed that the four system states,  $v_2$ ,  $v_3$ ,  $t_2$ , and  $t_3$  are measurable. In addition,  $t_1$ , and thus  $\tau_i$ , is measurable through (43).

B. Formulating the R2R Dry Transfer System as an APPLS with Bounded Modeling and Dwell-Time Uncertainty

This section presents how the R2R dry transfer dynamics naturally transform into an APPLS with bounded modeling and dwell-time uncertainties.

First, it is typical to define a physically realizable reference trajectory to regulate the system around. Define the following state, control, and exogenous input deviations:

$$\delta x(t) = x(t) - \tilde{x}(t), \delta u(t) = u(t) - \tilde{u}(t),$$
  

$$\delta w(t) = w(t) - \tilde{w}(t),$$
(49)

where  $\tilde{x}(t)$ ,  $\tilde{u}(t)$ , and  $\tilde{w}(t)$  represent the reference trajectory with desirable web tension and velocity characteristics. Using the piecewise nonlinear system dynamics (48) and LDI techniques like those outlined in [9], [11], the nonlinear system dynamics can be represented as follows.

$$\delta \dot{x} \in Co(\mathcal{A}_i)\delta x + B_i \delta u + B_{w_i} \delta w, \tag{50}$$

where  $\mathcal{A}_i = \left\{ \frac{\partial f_i}{\partial x_{X(t),u(t),w(t)}} \middle| t \in \left[ lT_P^* + t_{l,i-1}, lT_P^* + t_{l,i} \right) \right\}$ ,  $B_i = \frac{\partial f_i}{\partial u}$  is constant,  $B_{w_i} = \frac{\partial f_i}{\partial w}$  is treated as constant, and  $Co(\cdot)$  denotes the convex hull operator. (50) is called an LDI [9]–[11], [15]. If the following linear matrix inequality (LMI) is satisfied  $\forall \tilde{A}_{i,k} \in Co(\mathcal{A}_i)$ ,

$$V_i \ge 0$$
,  $W_i \ge 0$ , 
$$\begin{bmatrix} V_i & (\tilde{A}_{i,k} - A_i)^T \\ (\tilde{A}_{i,k} - A_i) & W_i \end{bmatrix} \ge 0$$
, (51)

then, when section i is being peeled,

$$\delta \dot{x}(t) = A_i \delta x(t) + B_i \delta u(t) + F_i \pi,$$
  

$$\pi(t)^T \pi(t) \le \left( G_i \delta x(t) \right)^T \left( G_i \delta x(t) \right),$$
(52)

where  $V_i = G_i^T G_i$  and  $W_i = F_i F_i^T$ . Also, the  $B_{w_i} \delta w$  term has been omitted since the reference trajectory  $\widetilde{w}(t)$  is assumed to be accurate. This method of transforming a nonlinear state

space system into a linear system with additive, unstructured, norm-bounded uncertainty has been summarized here. The benefit of this approach is that it allows control methods for linear systems with additive uncertainty to be used on nonlinear systems that operate within a known region in the state and input space. See [9]–[15] and the references therein for more details.

Next, the bounded dwell-time uncertainty will be quantified. Suppose that there is a dry transfer process with a constant unwinding speed  $v_1$  and sequentially numbered pattern sections, as in Figure 2. Let the closest and farthest position, relative to the beginning of the pattern, that section i can transition to section i+1 be denoted  $\underline{q_i}$  and  $\overline{q_i}$ , respectively. Thus, the minimum and maximum times that section i can transition to section i+1 are  $\underline{t_i} = lT_P^* + \frac{q_i}{v_1}/v_1$  and  $\overline{t_i} = lT_P^* + \overline{q_i}/v_1$ , respectively, where  $T_P^* = q_P/v_1$ ,  $q_P$  is the average length of the pattern, and l is the number of patterns that have been peeled since the process began .

Additionally, assume that the system is controlled using a set of state feedback matrices with a gain schedule such that  $K_i, K_{i,i+1}$ , or  $K_{i+1,i+1}$  is active when  $t \in |lT_P^* + \overline{t_{i-1}}, lT_P^* + \overline{t_{i-1}}|$  $\underline{t_i}$ ),  $\left[lT_P^* + \underline{t_i}, lT_P^* + t_{l,i}\right)$ , or  $\left[lT_P^* + t_{l,i}, lT_P^* + \overline{t_i}\right)$ , respectively. Note that switching the controller gain when a mode switch occurs is feasible in the R2R dry transfer case, since  $\tau_i$  is assumed to be constant and measurable, so it can be used to determine the active section. Thus, the switching times are unknown a-priori within the uncertain time region, but they are measurable in real time. Using this control strategy, (52) is equivalent to (1) and the stabilizing control results developed in Section 2.2 can be used to stabilize the R2R dry transfer system for patterned materials. This control-oriented modelling structure is more accurate than those of existing control designs that do not consider both dwell time and modeling uncertainty.

# C. Simulations of Dry Transfer of CVD Graphene

This section presents simulation results using the controller generated by Algorithm 1 to stabilize the dry transfer of CVD graphene from its copper growth substrate to a polymer target substrate, PVA [7], [24]. The web contains a series of CVD graphene sheets sandwiched between the growth substrate, the target substrate, and various adhesives. The graphene samples will alternate between long and short sizes. In addition, it is assumed that between the graphene sheets that are being transferred, the two PET transfer webs are laminated together in a similar manner as in [25]. Thus, one pattern, or period, will consist of four sections, or modes: an initial section of PET-PET laminated together, a long section of graphene, another section of PET-PET, and a short section of graphene. This simulation setup is illustrated in Figure 3. The modedependent parameters are given in Table 2. The physical parameter values were taken from [7], [24]. Three periods, or patterns, were simulated.

To ensure a statistically significant result, 100 simulations were conducted, with the switching events occurring randomly within the prescribed transition regions. Also, the initial conditions for each simulation were randomly generated to be near the reference trajectory. Figure 4 shows the norm of the

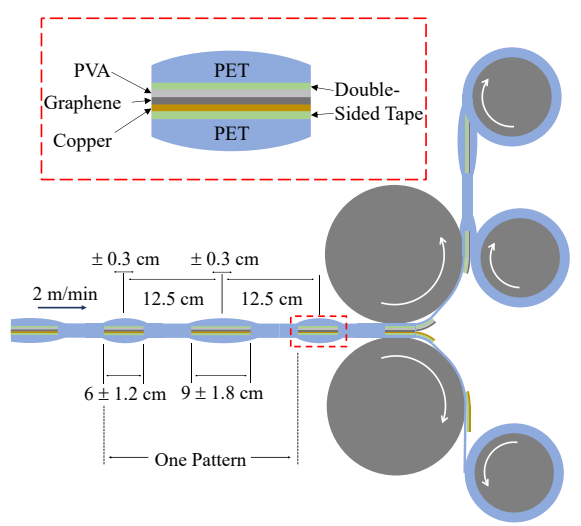


Figure 3. Simulation Setup

TABLE II. SYSTEM PARAMETERS

Section	Material	$\tau_i (J/m^2)$	$\underline{q_i}, \overline{q_i}$ (cm)	$\underline{t_i}, \overline{t_i}$ (s)
1	PET-PET	70	2.9, 5.3	0.88, 1.60
2	Graphene Stack	80	11.9, 14.3	3.60, 4.33
3	PET-PET	70	17.2, 19.0	5.21, 5.76
4	Graphene Stack	80	23.2, 25.0	7.03, 7.58

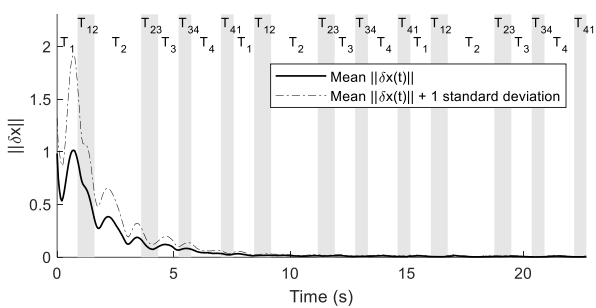


Figure 4. Norm of the state error over time

state error as defined in (49). The regions where the active mode is known and the transition regions where switching can occur are labeled and colored white and grey, respectively. The figure shows that the developed controller gains stabilize the R2R dry transfer system for patterned materials.

#### IV. CONCLUSION

This paper presents, for the first time, a stabilizing controller synthesis solution for APPLSs with both norm-bounded additive modeling uncertainty and dwell-time uncertainty. The utility of this modeling and control framework has been verified by using it to stabilize the R2R dry transfer system for patterned 2D materials with an exponential convergence rate. Future work will extend this framework to develop controllers with  $\mathcal{L}_2$ -gain performance guarantees, in addition to ensuring stability.

## REFERENCES

 G. E. Young and K. N. Reid, "Lateral and Longitudinal Dynamic Behavior and Control of Moving Webs," *J Dyn Syst Meas Control*, vol. 115, 1993.

- [2] J. Li, J. Fleetwood, W. B. Hawley, and W. Kays, "From Materials to Cell: State-of-the-Art and Prospective Technologies for Lithium-Ion Battery Electrode Processing," *Chemical Reviews*, vol. 122, no. 1. American Chemical Society, pp. 903–956, Jan. 12, 2022.
- [3] H. Zhou, W. Qin, Q. Yu, H. Cheng, X. Yu, and H. Wu, "Transfer printing and its applications in flexible electronic devices," *Nanomaterials*, vol. 9, no. 2, Feb. 2019.
- [4] P. Gupta et al., "A facile process for soak-and-peel delamination of CVD graphene from substrates using water," Sci Rep, vol. 4, Jan. 2014.
- [5] S. R. Na et al., "Selective mechanical transfer of graphene from seed copper foil using rate effects," ACS Nano, vol. 9, no. 2, pp. 1325– 1335, Feb. 2015.
- [6] H. Xin, Q. Zhao, D. Chen, and W. Li, "Roll-to-roll mechanical peeling for dry transfer of chemical vapor deposition graphene," J Micro Nanomanuf, vol. 6, no. 3, Sep. 2018.
- [7] N. Hong, D. Kireev, Q. Zhao, D. Chen, D. Akinwande, and W. Li, "Roll-to-Roll Dry Transfer of Large-Scale Graphene," *Advanced Materials*, vol. 34, no. 3, Jan. 2022.
- [8] J. Zhao et al., "Patterned Peeling 2D MoS2 off the Substrate," ACS Appl Mater Interfaces, vol. 8, no. 26, pp. 16546–16550, Jul. 2016.
- [9] S. P. Boyd, Linear matrix inequalities in system and control theory. Society for Industrial and Applied Mathematics, 1994.
- [10] C. R. Rodrigues, R. Kuiava, and R. A. Ramos, "Design of a linear quadratic regulator for nonlinear systems modeled via norm-bounded linear differential inclusions," *IFAC Proceedings Volumes*, vol. 44, no. 1, pp. 7352–7357, Jan. 2011.
- [11] R. Kuiava, R. A. Ramos, and H. R. Pota, "A New Approach for Modeling and Control of Nonlinear Systems Via Norm-Bounded Linear Differential Inclusions," 2012.
- [12] H. Hindi, C. Seong, and S. Boyd, "Computing Optimal Uncertainty Models from Frequency Domain Datal," *Conference on Decision and Control*, Dec. 2002.
- [13] M. Honda and P. Seiler, "Uncertainty Modeling for Hard Disk Drives," American Control Conference (ACC), 2014.
- [14] T. Asai, S. Hara, and T. Iwasaki, "Simultaneous parametric uncertainty modeling and robust control synthesis by LFT scaling," 2000
- [15] J. P. Folcher and L. El Ghaoui, "State-Feedback Design via Linear Matrix Inequalities: Application to a Benchmark Problem," Proceedings of IEEE International Conference on Control and Applications, 1994.
- [16] C. Martin, Q. Zhao, S. Bakshi, D. Chen, and W. Li, "H

  Optimal Control for Maintaining the R2R Peeling Front," in Modeling Estimation and Control Conference, 2022.
- [17] J. Tokarzewski, "Stability of periodically switched linear systems and the switching frequency," *Int J Syst Sci*, vol. 18, no. 4, pp. 697–726, 1987.
- [18] P. Li, J. Lam, and K. C. Cheung, "Stability, stabilization and L2-gain analysis of periodic piecewise linear systems," *Automatica*, vol. 61, pp. 218–226, Nov. 2015.
- [19] P. Li, J. Lam, Y. Chen, K. C. Cheung, and Y. Niu, "Stability and L2-gain analysis of periodic piecewise linear systems," in *Proceedings of the American Control Conference*, Institute of Electrical and Electronics Engineers Inc., Jul. 2015, pp. 3509–3514.
- [20] X. Xie, J. Lam, and C. Fan, "Robust time-weighted guaranteed cost control of uncertain periodic piecewise linear systems," *Inf Sci (N Y)*, vol. 460–461, pp. 238–253, Sep. 2018.
- [21] C. Fan, J. Lam, X. Xie, and P. Li, "Stability and Stabilization of Almost Periodic Piecewise Linear Systems With Dwell Time Uncertainty," *IEEE Trans Automat Contr*, vol. 68, no. 2, pp. 1130– 1137, Feb. 2023.
- [22] W. A. Coppel, Stability and asymptotic behavior of differential equations. in Heath mathematical monographs. Heath, 1965.
- [23] Y. Fang and T. G. Kincaid, "Stability Analysis of Dynamical Neural Networks," *IEEE Trans Neural Netw*, vol. I, no. 4, 1996.
- [24] N. Hong, Q. Zhao, D. Chen, K. M. Liechti, and W. Li, "A method to estimate adhesion energy of as-grown graphene in a roll-to-roll dry transfer process," *Carbon N Y*, vol. 201, pp. 712–718, Jan. 2023.
- [25] Q. Zhao, N. Hong, D. Chen, and W. Li, "A Dynamic System Model for Roll-to-Roll Dry Transfer of Two-Dimensional Materials and Printed Electronics," *Journal of Dynamic Systems, Measurement and Control, Transactions of the ASME*, vol. 144, no. 7, Jul. 2022.